# A note on computing heteroclinic trajectories of non-autonomous maps

Thorsten Hüls*
Department of Mathematics, Bielefeld University
POB 100131, 33501 Bielefeld, Germany
huels@math.uni-bielefeld.de

Yongkui Zou*‡
Department of Mathematics, Jilin University
Changchun 130012, P.R. China
zouyk@jlu.edu.cn

January 27, 2011

**Abstract**

We propose an adequate notion of a heteroclinic trajectory in non-autonomous systems that generalizes the notion of a heteroclinic orbit of an autonomous systems. A heteroclinic trajectory connects two families of semi-bounded trajectories that are bounded in backward and forward time. We apply boundary value techniques for computing one representative of each family. These approximations allow the construction of projection boundary conditions that enable the calculation of a heteroclinic trajectory with high accuracy. The resulting algorithm is applied to a non-autonomous version of Hénon's map.

**Keywords:** Non-autonomous discrete time dynamical systems, heteroclinic connection, numerical approximation, boundary value problems, error analysis.
**AMS Subject Classification:** 70K44, 34C37, 37B55.

## 1 Introduction

Homoclinic and heteroclinic orbits are important structures in dynamical systems. For example, the famous theorem of Smale, cf. [23], states that in au-

*Supported by CRC 701 'Spectral Structures and Topological Methods in Mathematics'.
‡Supported by NSFC No. 10671082.

tonomous systems, the dynamics in a neighborhood of a homoclinic orbit is chaotic. In autonomous systems, heteroclinic orbits describe possible transitions between two equilibria; consequently they lie in the intersection of the unstable manifold of the first equilibrium with the stable manifold of the second one.

To avoid the expensive computation of invariant manifolds [19], various approximation results for directly computing these orbits have been developed in the literature. For this task boundary value approaches turn out to be very efficient. In continuous time, cf. [1], the resulting algorithms are implemented, for example, in the current version of the bifurcation toolbox MATCONT [7, 10]. For discrete time systems, we refer to [2, 3, 5, 14].

Real-life systems, like population models in a fluctuating environment [8, 9, 4], are typically non-autonomous. This fact motivates the consideration of non-autonomous difference equations of the form

$$x_{n+1} = f_n(x_n), \quad n \in \mathbb{Z}, \tag{1}$$

where $f_n \in \mathcal{C}^\infty(\mathbb{R}^k, \mathbb{R}^k)$ are assumed to be diffeomorphisms for all $n \in \mathbb{Z}$. In this setup, homoclinic and heteroclinic orbits lie in the intersection of stable and unstable fiber bundles which are non-autonomous analogs of invariant manifolds, see [13, 24, 22].

Consequently, a homoclinic orbit w.r.t. a fixed point from the autonomous world has to be replaced by a pair of trajectories $\bar{\xi}_{\mathbb{Z}} := \{\bar{\xi}_n\}_{n\in\mathbb{Z}}$ and $\bar{z}_{\mathbb{Z}} := \{\bar{z}_n\}_{n\in\mathbb{Z}}$ of (1), converging towards each other, i.e. $\lim_{n\to\pm\infty} \|\bar{\xi}_n - \bar{z}_n\| = 0$. Pairs of homoclinic trajectories are analyzed in [15, 18].

In this paper we extend these ideas to the non-autonomous analog of a heteroclinic connection between two fixed points, which we call a heteroclinic trajectory. This is an orbit of (1), connecting two trajectories $\bar{\xi}^-_{\mathbb{Z}}$ and $\bar{\xi}^+_{\mathbb{Z}}$ that are bounded in backward and forward time, respectively. First, one needs approximations of the reference trajectories $\bar{\xi}^\pm_{\mathbb{Z}}$. These reference trajectories are not unique due to our weak assumption of semi-boundedness and consequently, two families of semi-bounded trajectories exit. We assume that the corresponding variational equations

$$\begin{aligned} u_{n+1} &= Df_n(\bar{\xi}^-_n)u_n, \quad n \in \mathbb{Z}^-, \\ v_{n+1} &= Df_n(\bar{\xi}^+_n)v_n, \quad n \in \mathbb{Z}^+ \end{aligned}$$

have half-sided exponential dichotomies, cf. Appendix A. This hyperbolicity assumption justifies numerical computations. It turns out that all trajectories of the semi-bounded family on $\mathbb{Z}^+$ converge towards each other exponentially fast in forward time, and the same holds true in negative time for the second family. We impose an initial condition to select one representative of each family and state a theorem that guarantees an accurate numerical approximation. Essentially, we make use of the fact that under hyperbolicity assumptions, errors

from the boundary, decay exponentially fast toward the midpoint of the finite computational interval.

In a second step, these orbits are used to set up the boundary operator for computing a heteroclinic trajectory. For this purpose, we take linear approximations of stable and unstable fiber bundles that we obtain by computing dichotomy projectors, using techniques that have been developed in [16, 17].

We illustrate the approximation results for the first step by computing several semi-bounded trajectories of a non-autonomous version of Hénon's map. In a second step, we solve the corresponding boundary value problem and get the desired heteroclinic connection between these non-autonomous families of semi-bounded trajectories.

# 2 Heteroclinic trajectories

We start this section be introducing the concept of heteroclinic trajectories. Then an algorithm for computing these objects is proposed.

Denote by $X_J$ the space of bounded sequences on $J$:

$$X_J := \left\{ u_J = (u_n)_{n\in J} \in (\mathbb{R}^k)^J : \sup_{n\in J} \|u_n\| < \infty \right\}$$

equipped with the $\ell_\infty$-norm, and denote by $0_J$ the zero element in $X_J$.

Consider a non-autonomous difference equations that is generated by a parameter-dependent map

$$x_{n+1} = f(x_n, \lambda_n), \quad n \in \mathbb{Z}. \tag{2}$$

We impose the following assumptions on $f$.

**A1** $f \in \mathcal{C}^\infty(\mathbb{R}^k \times \mathbb{R}, \mathbb{R}^k)$ and $f(\cdot, \lambda)$ is a diffeomorphism for all $\lambda \in \mathbb{R}$.

**A2** For the parameter sequence $\bar{\lambda}_\mathbb{Z}$, equation (2) has two semi-bounded solutions $\bar{\xi}^+_\mathbb{Z} = \{\bar{\xi}^+_n\}_{n\in\mathbb{Z}}$ and $\bar{\xi}^-_\mathbb{Z} = \{\bar{\xi}^-_n\}_{n\in\mathbb{Z}}$ which are bounded for $n \geq 0$ and $n \leq 0$, respectively.

**A3** The variational equations

$$u_{n+1} = D_x f(\bar{\xi}^-_n, \bar{\lambda}_n) u_n, \quad n \in \mathbb{Z}^-, \tag{3}$$
$$u_{n+1} = D_x f(\bar{\xi}^+_n, \bar{\lambda}_n) u_n, \quad n \in \mathbb{Z}^+ \tag{4}$$

possess exponential dichotomies on $\mathbb{Z}^-$ and $\mathbb{Z}^+$, respectively, with data $(K^\pm, \alpha^\pm_s, \alpha^\pm_u, P^{\pm s}_{\mathbb{Z}^\pm}, P^{\pm u}_{\mathbb{Z}^\pm})$, cf. Appendix A, Definition 9.

Denote by $k^\pm_s$ and $k^\pm_u$ the dimensions of the subspaces $\mathcal{R}(P^{\pm s}_n)$ and $\mathcal{R}(P^{\pm u}_n)$, respectively.

**Definition 1** *Fix $\lambda_{\mathbb{Z}}$ and let $\xi^{\pm}_{\mathbb{Z}}$ and $z_{\mathbb{Z}}$ be three different solutions of the non-autonomous difference equation* (2)*. The trajectory $z_{\mathbb{Z}}$ is* ***heteroclinic*** *with respect to $\xi^{+}_{\mathbb{Z}}$ and $\xi^{-}_{\mathbb{Z}}$, if*

$$\lim_{n\to+\infty} \|z_n - \xi^+_n\| = 0 \quad \text{and} \quad \lim_{n\to-\infty} \|z_n - \xi^-_n\| = 0.$$

**A4** For the parameter sequence $\bar{\lambda}_{\mathbb{Z}}$, equation (2) possesses a heteroclinic trajectory $\bar{z}_{\mathbb{Z}}$ with respect to $\bar{\xi}^{+}_{\mathbb{Z}}$ and $\bar{\xi}^{-}_{\mathbb{Z}}$.

Note that it follows from the Roughness-Theorem 10 that the variational equation

$$u_{n+1} = D_x f(\bar{z}_n, \bar{\lambda}_n) u_n, \quad n \in \mathbb{Z} \tag{5}$$

has exponential dichotomies on $\mathbb{Z}^-$ and on $\mathbb{Z}^+$. Denote be $Q^{\pm s,u}_n$ the corresponding projectors. If $k^-_u + k^+_s = k$, then half sided dichotomies can be combined to a dichotomy on $\mathbb{Z}$, if $\mathcal{R}(Q^{-u}_0) \oplus \mathcal{R}(Q^{+s}_0) = \mathbb{R}^k$, cf. [21].

## 2.1 An alternative viewpoint

For achieving a deeper understanding and to see that the above assumptions are in certain respects minimal, we look at heteroclinic orbits from an alternative viewpoint. Consider a trajectory $\bar{z}_{\mathbb{Z}}$, having an exponential dichotomy on $\mathbb{Z}$ with at least one stable and one unstable direction. Denote by $\Psi$ the solution operator of (2) with parameter sequence $\bar{\lambda}_{\mathbb{Z}}$. The stable and unstable fibers of $\bar{z}_{\mathbb{Z}}$ are defined as

$$\begin{aligned} S^s_0(\bar{z}_{\mathbb{Z}}) &= \{x \in \mathbb{R}^k : \lim_{n\to\infty} \|\Psi(n,0)x - \bar{z}_n\| = 0\}, \\ S^u_0(\bar{z}_{\mathbb{Z}}) &= \{x \in \mathbb{R}^k : \lim_{n\to-\infty} \|\Psi(n,0)x - \bar{z}_n\| = 0\}. \end{aligned}$$

Any trajectory $\xi^+_{\mathbb{Z}}$ which starts on the stable fiber bundle at time $n = 0$ converges in forward time exponentially fast towards $\bar{z}_{\mathbb{Z}}$. Similarly, any starting point on the unstable fiber bundle results in a trajectory $\xi^-_{\mathbb{Z}}$ that converges in backwards time towards $\bar{z}_{\mathbb{Z}}$.

From the Roughness-Theorem 10, it follows that the variational equations along $\xi^-_{\mathbb{Z}}$ and $\xi^+_{\mathbb{Z}}$ have exponential dichotomies on $\mathbb{Z}^-$ and $\mathbb{Z}^+$, respectively, cf. **A4**. Furthermore, $\xi^-_{\mathbb{Z}}$ is generically not bounded in forward time and $\xi^+_{\mathbb{Z}}$ is not bounded in backward time. This is assumed in **A2**. From this viewpoint it is also clear, that these orbits are not unique, since each starting point in the corresponding fiber $S^{s,u}_0(\bar{z}_{\mathbb{Z}})$ leads to a semi-bounded trajectory.

Uniqueness of the semi-bounded trajectories $\bar{\xi}^{\pm}_{\mathbb{Z}}$ can only be achieved by introducing an extra condition, for example, by taking initial points from the intersection of the fiber $S^{s,u}_0(\bar{z}_{\mathbb{Z}})$ with a hyperplane $\Sigma^{s,u}_0$, cf. Figure 1.

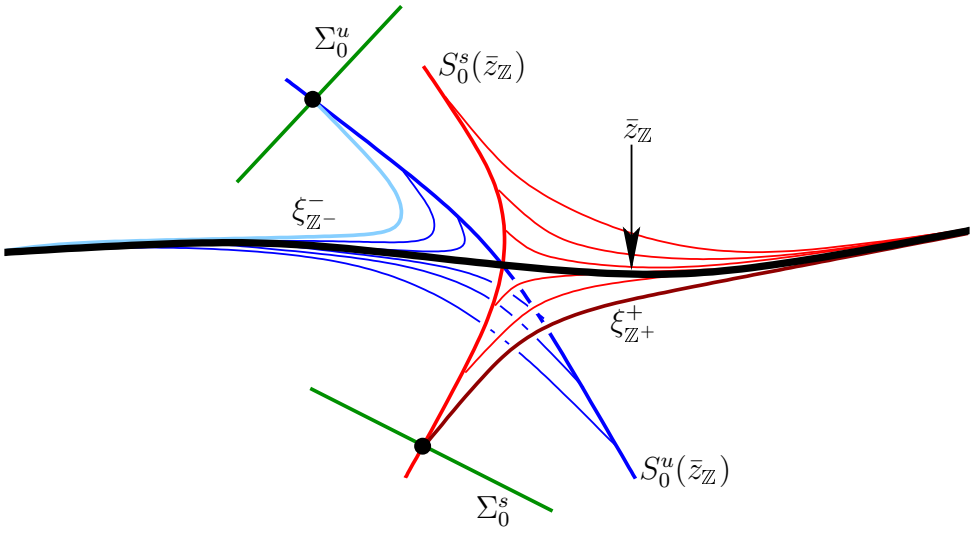


Figure 1: *Illustration of families of bounded trajectories on $\mathbb{Z}^{\pm}$ that start on the stable and unstable fiber $S_0^{s,u}(\bar{z}_{\mathbb{Z}})$, respectively. The intersection of $S_0^{s,u}(\bar{z}_{\mathbb{Z}})$ with the hyperplane $\Sigma_0^{s,u}$ gives locally unique orbits.*

## 2.2 Initial conditions for bounded trajectories

Consider solutions that are bounded in forward time on the interval $[n_0, \infty) \cap \mathbb{Z}$. We impose the following assumption on the hyperplane $\Sigma^s_{n_0}$:

**A5** Let $\Sigma^s_{n_0}$ be a $k_u^+$-dimensional subspace, such that $\Sigma^s_{n_0} \oplus \mathcal{R}(P^{+s}_{n_0}) = \mathbb{R}^k$.

Note that a generic subspace of dimension $k_u^+$ satisfies this assumption.

The initial condition $x_{n_0} \in \Sigma^s_{n_0}$ can equivalently be written as

$$(Y^+_{n_0})^T x_{n_0} = 0, \tag{6}$$

where the columns of $Y^+_{n_0}$ form a basis of the orthogonal complement of $\Sigma^s_{n_0}$.

Define the discrete intervals $J_+ = [n_0, n_+] \cap \mathbb{Z}$ and $\tilde{J}_+ = [n_0, n_+ - 1] \cap \mathbb{Z}$, where $0 \leq n_0 < n_+$ and the case $n_+ = +\infty$ is included.

Let $\lambda_{J_+}$ be a fixed sequence. We combine the two conditions (2) and (6) for computing an orbit that starts in $\Sigma^s_{n_0}$ by introducing the operator $\Gamma^+_{J_+}$:

$$\begin{array}{rccl} \Gamma^+_{J_+}: & X_{J_+} \times \mathbb{R}^{J_+} & \to & X_{\tilde{J}_+} \times \mathbb{R}^{k_s^+} \\ & (x_{J_+}, \lambda_{J_+}) & \mapsto & ((x_{n+1} - f(x_n, \lambda_n))_{n \in \tilde{J}_+}, (Y^+_{n_0})^T x_{n_0}). \end{array}$$

In case $J_+ = \mathbb{Z}^+$, the next lemma shows that, by assuming **A5**, a zero of $\Gamma^+_{\mathbb{Z}^+}$ is regular, which implies local uniqueness of the solution of equation (2) with initial condition (6) on $\mathbb{Z}^+$.

**Lemma 2** *Assume **A1**–**A3** and **A5** with $n_0 = 0$. Then $\bar{\xi}^+_{\mathbb{Z}^+}$ is a regular solution of*

$$\Gamma^+_{\mathbb{Z}^+}(x_{\mathbb{Z}^+}, \bar{\lambda}_{\mathbb{Z}^+}) = 0_{\mathbb{Z}^+}. \tag{7}$$

**Proof:** Regularity means that the linear operator

$$D_{x_{\mathbb{Z}^+}}\Gamma(\bar{\xi}^+_{\mathbb{Z}^+}, \bar{\lambda}_{\mathbb{Z}^+}) : X_{\mathbb{Z}^+} \to X_{\mathbb{Z}^+} \times \mathbb{R}^{k^+_s} \tag{8}$$

is a homeomorphism, i.e.

$$D_{x_{\mathbb{Z}^+}}\Gamma(\bar{\xi}^+_{\mathbb{Z}^+}, \bar{\lambda}_{\mathbb{Z}^+})u_{\mathbb{Z}^+} = (r_{\mathbb{Z}^+}, v) \tag{9}$$

has for any $r_{\mathbb{Z}^+} \in X_{\mathbb{Z}^+}$ and $v \in \mathbb{R}^{k^+_s}$ a unique solution. Note that system (9) is equivalent to

$$\begin{aligned} u_{n+1} - D_x f(\bar{\xi}^+_n, \bar{\lambda}_n)u_n &= r_n, \quad n \geq 0, \\ (Y^+_0)^T u_0 &= v. \end{aligned} \tag{10}$$

By [21, Lemma 2.7], we obtain a unique bounded solution $u_{\mathbb{Z}^+} \in X_{\mathbb{Z}^+}$ of equation (10) by fixing $P^{+s}_0 u_0$. Note that the linear equation

$$(Y^+_0)^T P^{+s}_0 u_0 = v$$

is uniquely solvable due to the regularity of the matrix $(Y^+_0)^T{}_{|\mathcal{R}(P^{+s}_0)}$, see Assumption **A5**. As a consequence, the operator (8) is one to one and onto.

■

By choosing a subspace $\Sigma^s_{n_0}$ that satisfies **A5**, we set up the boundary condition (6), and uniquely obtain a bounded trajectory, starting on the stable fiber $S^s_0(\bar{z}_{\mathbb{Z}})$. Typically, this is not the trajectory $\bar{\xi}^+_{\mathbb{Z}^+}$ from Assumption **A2**. All starting points $x_0 \in S^s_0(\bar{z}_{\mathbb{Z}})$ define trajectories $x_{\mathbb{Z}}$ that converge towards $\bar{z}_{\mathbb{Z}}$ as $n \to \infty$. Furthermore, one immediately sees by using the Roughness-Theorem 10 that the variational equation

$$u_{n+1} = D_x f(x_n, \bar{\lambda}_n)u_n \tag{11}$$

has an exponential dichotomy on $J = [N, \infty)$, since

$$\|D_x f(x_n, \bar{\lambda}_n) - D_x f(\bar{\xi}^+_n, \bar{\lambda}_n)\| \leq \beta$$

for sufficiently large $N$, where $\beta$ denotes the bound for the perturbation in Theorem 10. The resulting dichotomy of (11) can be extended to $\mathbb{Z}^+$ by adjusting the constant $K$.

Note that the difference between these solutions $d_n = x_n - \bar{\xi}^+_n$ converges exponentially fast to 0 as $n \to \infty$, since the difference equation

$$d_{n+1} = f(\bar{\xi}^+_n + d_n, \bar{\lambda}_n) - f(\bar{\xi}^+_n, \bar{\lambda}_n) = \int_0^1 D_x f(\bar{\xi}^+_n + \tau d_n, \bar{\lambda}_n)d\tau \cdot d_n \tag{12}$$

has by the Roughness-Theorem 10 an exponential dichotomy on $\mathbb{Z}^+$ with slightly changed data $(\tilde{K}, \tilde{\alpha}_s^+, \tilde{\alpha}_u^+, \tilde{P}_{\mathbb{Z}^+}^{+s}, \tilde{P}_{\mathbb{Z}^-}^{+u})$. Denote by $\tilde{\Phi}$ the solution operator of (12), then it follows that

$$\|d_n\| = \|\tilde{\Phi}(n,0)d_0\| = \|\tilde{\Phi}(n,0)\tilde{P}_0^{+s}d_0\| \leq \tilde{K}\mathrm{e}^{-\tilde{\alpha}_s^+ n}\|d_0\|.$$

By reversing the time, we get a similar exponential estimate for the second trajectory $\bar{\xi}_{\mathbb{Z}^-}^-$.

From this viewpoint, the orbit $\bar{z}_{\mathbb{Z}}$ is heteroclinic with respect to two families of trajectories; one that converges in forward time and another one that converges in backward time towards $\bar{z}_{\mathbb{Z}}$ with exponential rates.

# 3 Numerical approximation of semi-bounded trajectories

We now return to the original viewpoint and introduce an algorithm which gives accurate approximations of the two semi-bounded trajectories $\bar{\xi}_{\mathbb{Z}}^{\pm}$. In a second step we then compute in Section 4 a heteroclinic connection $\bar{z}_{\mathbb{Z}}$ of these trajectories.

We assume without loss of generality that $\bar{\xi}_{\mathbb{Z}}^+$ from Assumption **A2** additionally satisfies the initial condition (6). Note that the trajectory $\bar{\xi}_{\mathbb{Z}}^+$ is "only" a representative of the family of hyperbolic trajectories with same asymptotic behavior, in forward time.

We derive an approximation result for $\bar{\xi}_{\mathbb{Z}}^+$. The case of semi-bounded trajectories in negative time can be treated similarly. Assume that the subspace $\Sigma_0^s$ is fixed such that **A5** holds.

By Lemma 2, $\bar{\xi}_{\mathbb{Z}}^+$ is a regular zero of $\Gamma_{\mathbb{Z}^+}^+$ at the parameter $\bar{\lambda}_{\mathbb{Z}^+}$. The implicit function theorem guarantees the existence of convex neighborhoods $U = U(\bar{\lambda}_{\mathbb{Z}^+})$ and $V = V(\bar{\xi}_{\mathbb{Z}^+})$ such that for each $\mu_{\mathbb{Z}^+} \in U$ it follows that $\Gamma_{\mathbb{Z}^+}^+(\cdot, \mu_{\mathbb{Z}^+})$ has a unique zero in $V$.

## 3.1 Extension of semi-bounded trajectories to bounded trajectories on $\mathbb{Z}$

For proving error estimates for numerically computed semi-bounded trajectories, we use an approximation theorem for bounded trajectories on $\mathbb{Z}$ which was developed in [18], see Appendix B, Theorem 11. To make this result applicable, we first change the system (2) to

$$x_{n+1} = g(x_n, \lambda_n), \quad n \in \mathbb{Z} \tag{13}$$

such that the following condition is satisfied.

**C1** Let $x_{\mathbb{Z}}$ be a bounded solution of (13) on $\mathbb{Z}$. Then $\xi_n := x_n$, $n \in \mathbb{Z}^+$ defines a bounded solution of (2) on $\mathbb{Z}^+$ that satisfies the initial condition (6).

Consequently, an accurate approximation of $x_{\mathbb{Z}}$ of (13) immediately gives an accurate approximation of $\xi^+_{\mathbb{Z}^+}$ on $\mathbb{Z}^+$.

Assume **A1-A5** and let the columns of $X^s$ and $X^u$ form bases of $\mathcal{R}(P_0^{+s})$ and of $\Sigma_0^s$, respectively. Then, the matrix $S = [X^s, X^u]$ is by Assumption **A5** regular. Define

$$g(x, \lambda_n) := \begin{cases} f(x, \lambda_n) & \text{for } n \geq 0, \\ S \begin{pmatrix} \mathrm{e}^{-\alpha_s} I_{k_s^+} & 0 \\ 0 & \mathrm{e}^{\alpha_u} I_{k_u^+} \end{pmatrix} S^{-1} x & \text{for } n < 0. \end{cases} \tag{14}$$

Note that $g$ depends on the dichotomy rates and the projectors from **A3**, which are a-priori not known. Introducing this system merely has technical reasons. Indeed, this extended system makes approximation results for bounded trajectories on $\mathbb{Z}$ from [18], cf. Appendix B, applicable to semi-bounded trajectories.

**Lemma 3** *With the above assumptions, condition **C1** holds true for $g$, defined in* (14).

**Proof:** Let $x_{\mathbb{Z}}$ be a bounded solution of (13). Obviously, $\xi_{\mathbb{Z}^+} := x_{\mathbb{Z}^+}$ is a bounded solution of (2) on $\mathbb{Z}^+$. It remains to prove that the boundary condition (6) holds true. Due to the boundedness of $x_{\mathbb{Z}}$ as $n \to -\infty$ it follows that $x_0$ has no component in $X^s$; otherwise this solution increases exponentially fast in backward time. Thus $x_0 = X^u \gamma$ with some $\gamma \in \mathbb{R}^{k_u^+}$ and consequently $x_0 \in \Sigma_0^s$, which is equivalent to $(Y_0^+)^T x_0 = 0$.

■

Consequently, regular solutions of (7) give regular bounded trajectories of (14). Denote by $\bar{x}_{\mathbb{Z}}$ the $g(\cdot, \bar{\lambda})$-orbit that satisfies $\bar{x}_{\mathbb{Z}^+} = \bar{\xi}^+_{\mathbb{Z}^+}$. We use the same notation $U$ and $V$ for neighborhoods of $\bar{x}_{\mathbb{Z}}$ and $\bar{\lambda}_{\mathbb{Z}}$ on $\mathbb{Z}$ such that for $\lambda_{\mathbb{Z}} \in U$ there exists a unique bounded trajectory $x_{\mathbb{Z}} \in V$ of (14).

## 3.2 Errors on finite intervals; an algorithm for computing accurate approximations of semi-bounded trajectories

We already have seen that semi-bounded solutions on $\mathbb{Z}^+$ of the original system (7) correspond to bounded trajectories of the extended system (14). In this section, a boundary value approach is applied to the latter system (14) for obtaining approximations numerically. Projection boundary conditions are particularly useful, since the left boundary condition is known exactly and given by our initial condition (6). At the right boundary, we only can guess an appropriate condition.

First, errors are analyzed that occur when we alter the system at the right boundary.

**Theorem 4** *Assume **A1**-**A3** and **A5**. Let $\mu_{\mathbb{Z}} \in U$ be a sequence of parameters such that $\mu_n = \bar{\lambda}_n$ for all $n \leq n_+$. Denote by $x_{\mathbb{Z}}$, $y_{\mathbb{Z}} \in V$ the corresponding solutions of $x_{n+1} = g(x_n, \bar{\lambda}_n)$ and $y_{n+1} = g(y_n, \mu_n)$, respectively. Then*

$$\|y_n - x_n\|_\infty \leq C\mathrm{e}^{-\alpha_u^+(n_+-n)} \quad \textit{for } n \leq n_+.$$

The proof immediately follows from [18, Theorem 5].

Consequently, errors that occur due to an inaccurate right boundary condition decay exponentially fast towards the left side. We construct a boundary operator by picking a subspace $\Sigma_{n_+}^u$ of dimension $k_u^+$ at random. Let the columns of $Y_{n_+}^+$ form a basis of $(\Sigma_{n_+}^u)^\perp$, then

$$b: \begin{array}{ccc} \mathbb{R}^k \times \mathbb{R}^k & \to & \mathbb{R}^k \\ (x_0, x_{n_+}) & \mapsto & \begin{pmatrix} (Y_0^+)^T x_0 \\ (Y_{n_+}^+)^T x_{n_+} \end{pmatrix} . \end{array} \tag{15}$$

We assume that for sufficiently large $n_+$, we can alter the sequence of parameters $\bar{\lambda}_{\mathbb{Z}}$ such that the solution with respect to this new parameter sequence satisfies the right boundary condition.

**A6** Let $\Sigma_{n_+}^u$ be a subspace of dimension $k_u^+$ such that

$$\measuredangle(\Sigma_{n_+}^u, \mathcal{R}(P_{n_+}^u)) > \sigma. \tag{16}$$

Denote by $Y_{n_+}^+$ a basis of $(\Sigma_{n_+}^u)^\perp$. Let $\mu_{\mathbb{Z}} \in U$ be a sequence with $\mu_n = \bar{\lambda}_n$ for $n \leq n_+$, such that the unique bounded solution $\tilde{x}_{\mathbb{Z}} \in V$ of

$$x_{n+1} = g(x_n, \mu_n), \quad n \in \mathbb{Z}$$

satisfies $(Y_{n_+}^+)^T \tilde{x}_{n_+} = 0$.

Note that **A6** is a strong assumption that is not automatically satisfied for randomly chosen $\Sigma_{n_+}^u$. In particular, it is not clear whether this subspace has an intersection with the neighborhood $V$. However, if a good approximation $\xi$ of $x_{n_+}$ is known a-priori, one can shift the boundary condition by replacing $x_{n_+}$ by $(x_{n_+} - \xi)$ in the right side of (15) and get rid of the latter problem. Moreover, the angle condition (16) is typically satisfied for randomly chosen subspaces, and $\tilde{x}_{\mathbb{Z}}$ exists for our nonlinear examples.

The following approximation result on the finite interval $J = [0, n_+]$ is a consequence of Appendix B, Theorem 11.

**Theorem 5** *Assume **A1**-**A3** and **A5**. Fix $\sigma > 0$ and a sufficiently large $n_+$ and choose a subspace $\Sigma_{n_+}^u$ and a sequence $\mu_{\mathbb{Z}}$ with corresponding solution $\tilde{x}_{\mathbb{Z}}$, such that **A6** is satisfied.*

*Then, there exists a $\delta > 0$ such that the boundary value problem*

$$x_{n+1} = f(x_n, \bar{\lambda}_n), \quad n \in [0, n_+ - 1]$$

*with boundary operator* (15) *has a unique solution $y_J$ in the $\delta$-neighborhood $B_\delta(\tilde{x}_J)$. Furthermore, these solutions coincide on the finite interval $J$, i.e. $y_J = \tilde{x}_J$.*

**Proof:** A careful inspection of the proof of [18, Theorem 4] reveals that the choice of $n_+$ only depends on the dichotomy rates and on the angle between the subspace $\Sigma^u_{n_+}$ and $\mathcal{R}(P^u_{n_+})$. Note that we have uniform estimates of dichotomy rates, for parameter sequences and $g$-orbits in our neighborhoods $U$ and $V$.

Since the solution $\tilde{x}_\mathbb{Z}$ satisfies the boundary condition (15), we get no approximation error inside the interval $J$.

■

A combination of the previous results allows the approximation of the original trajectory $\bar{x}_\mathbb{Z}$ up to any given accuracy.

**Theorem 6** *Assume **A1**-**A3** and **A5**, **A6**. For any tolerance $\Delta > 0$ there exist constants $n_+ < N \in \mathbb{N}$ and a $\delta > 0$ such that the boundary value problem*

$$y_{n+1} = f(y_n, \bar{\lambda}_n), \quad n \in [0, N-1] \tag{17}$$

*with boundary condition* (15) *has a unique solution $y_{[0,N]} \in B_\delta(\bar{x}_{[0,N]})$ that satisfies*

$$\|\bar{x}_n - y_n\| \leq \Delta \quad \textit{for all } 0 \leq n \leq n_+.$$

**Proof:** By Theorem 5, the boundary value problem (17) has for sufficiently large $N$ a unique solution $y_N \in B_\delta(\bar{x}_{[0,N]})$ that coincides with the trajectory $\tilde{x}_{[0,N]}$ from Assumption **A6**.

Using Theorem 4 we obtain for $0 \leq n \leq N$

$$\|\bar{x}_n - y_n\| = \|\bar{x}_n - \tilde{x}_n\| \leq C\mathrm{e}^{-\alpha^+_u(N-n)}.$$

Thus, for $N$ sufficient large we find an $n_+ < N$ such that $C\mathrm{e}^{-\alpha^+_u(N-n)} < \Delta$ for all $0 \leq n \leq n_+$.

■

Summarizing these results, we obtain the following algorithm for computing an accurate approximation of the semi-bounded trajectory $\bar{\xi}^+_\mathbb{Z}$. First, choose the initial condition (6) and an appropriate boundary condition on the right side. Then, solve the boundary value problem (17), (15) on a buffer interval $[0, N]$. Finally, the left part of the solution from 0 to $n_+$ gives an accurate approximation of the semi-bounded trajectory $\bar{\xi}_{\mathbb{Z}^+}$.

### 3.3 Numerical experiments: Computation of semi-bounded trajectories

For numerical experiments, we choose a non-autonomous version of the well known Hénon map, see [12, 20, 6, 11], which is defined as

$$f(x,\lambda) = \begin{pmatrix} 1 + x_2 - \lambda x_1^2 \\ 1.4 x_1 \end{pmatrix}.$$

For constant parameter sequences $\lambda_n = \lambda$, $n \in \mathbb{Z}$, the system

$$x_{n+1} = f(x_n, \lambda_n), \quad n \in \mathbb{Z}$$

is autonomous and has for $\lambda > -\frac{1}{25}$ two fixed points

$$\eta_\pm(\lambda) = \begin{pmatrix} \nu(\lambda) \\ 1.4\nu(\lambda) \end{pmatrix}, \quad \text{where } \nu(\lambda) = \frac{1}{5\lambda}\left(1 \pm \sqrt{1+25\lambda}\right).$$

Passing over to the non-autonomous case $\lambda_n = \lambda + \varepsilon r_n$ with a randomly chosen sequence $r_\mathbb{Z} \in [-1,1]^\mathbb{Z}$ we obtain for sufficiently small $\varepsilon$ two bounded trajectories $\xi^\pm_\mathbb{Z}(\lambda_\mathbb{Z})$ on $\mathbb{Z}$, and consequently, there exist two families of semi-bounded trajectories.

We demonstrate the numerical approximation of $\bar{\xi}^+_\mathbb{Z}(\lambda_\mathbb{Z})$ on the finite interval $J = [0, 100]$ for the parameters $\lambda_n = 0.4 + \varepsilon r_n$ with $\varepsilon = 0.5$. We numerically solve the boundary value problem (17), (15) using Newton's method. As initial guess of the solution, we take the fixed point $\eta_+(0.4)$. The boundary operator $Y^+_{n_+}$ is chosen according the unstable subspace of $\eta_+(0.4)$. For emphasizing the influence of the initial condition on the solution, we solve the boundary value problem for various initial planes $\Sigma^s_0$ and plot the solutions in Figures 2 and 3 in case Newton's method converges. In these figures, one can clearly observe the convergence of the solutions towards each other. Assuming **A5**, each initial plane $\Sigma^s_0$ contains at least one point of the stable fiber $S^s_0(\bar{\xi}^+_\mathbb{Z}(\lambda_\mathbb{Z}))$. A plot of the solutions for various initial planes automatically gives an approximation of this fiber bundle.

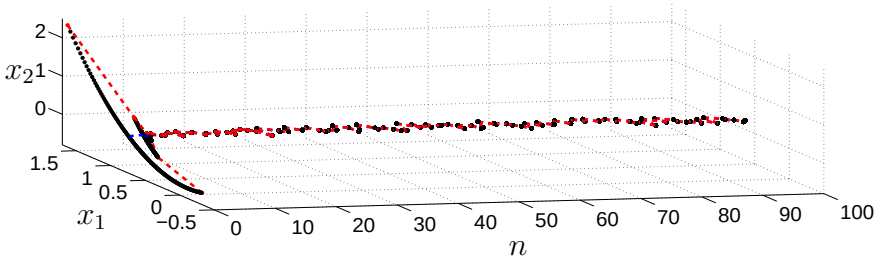


Figure 2: *Semi-bounded trajectories, computed on the interval* $[0, 100]$ *for various initial conditions.*

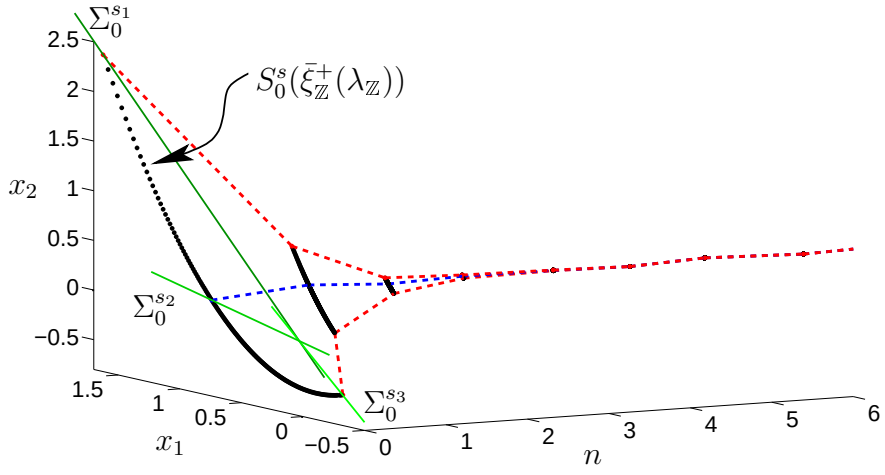


Figure 3: *Semi-bounded trajectories, computed on the interval* $[0, 100]$ *for various initial conditions, where only the first 7 points of each orbit are displayed. The orbits that start on the green subspaces* $\Sigma_0^{s_i}$, $i \in \{1, 2, 3\}$ *are connected with dotted lines.*

Approximations of the second trajectory $\bar{\xi}_{\mathbb{Z}}^-(\lambda)$ on $\mathbb{Z}^-$ are given in Figure 4, together with the trajectories from Figure 2. Observe that the stable and unstable fibers $S_0^s(\bar{\xi}_{\mathbb{Z}}^+(\lambda_{\mathbb{Z}}))$ and $S_0^u(\bar{\xi}_{\mathbb{Z}}^-(\lambda_{\mathbb{Z}}))$ intersect transversally. Therefore, a heteroclinic connection of these trajectories exists for which we propose an approximation routine in the forthcoming section.

# 4 Approximation of heteroclinic trajectories

With the results from the previous sections, we get accurate approximations of the semi-bounded trajectories $\bar{\xi}_{\mathbb{Z}^\pm}^\pm$. These approximations are needed for the definition of accurate boundary conditions that are essential for the computation of the heteroclinic trajectory $\bar{z}_{\mathbb{Z}}$.

First we ensure that the variational equation along the heteroclinic trajectory (5) possesses an exponential dichotomy by assuming the following transversality condition.

**A7** $k_u^- + k_s^+ = k$ and the trajectory $\bar{z}_{\mathbb{Z}}$ is transversal, i.e.

$$u_{n+1} = D_x f(\bar{z}_n, \bar{\lambda}_n) u_n,\ n \in \mathbb{Z},\ u_{\mathbb{Z}} \in X_{\mathbb{Z}} \quad \Longleftrightarrow \quad u_{\mathbb{Z}} = 0_{\mathbb{Z}}.$$

**Lemma 7** *Assume* ***A1-A4*** *and* ***A7****. Then the difference equation* (5) *has an exponential dichotomy on* $\mathbb{Z}$.

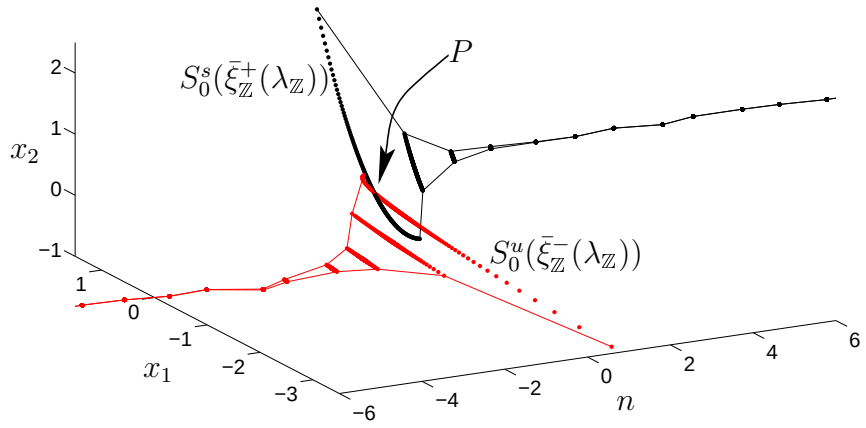


Figure 4: *Semi-bounded trajectories, computed on the interval* $[-100, 0]$ *(in red) and on* $[0, 100]$ *(in black) for various initial conditions, where only the first 7 points of each orbit are displayed.* $P$ *denotes an intersection of the stable and unstable fibers* $S_0^s(\bar{\xi}_{\mathbb{Z}}^+(\lambda_{\mathbb{Z}}))$ *and* $S_0^u(\bar{\xi}_{\mathbb{Z}}^-(\lambda_{\mathbb{Z}}))$.

**Proof:** From the convergence $\lim_{n\to\infty} \|\bar{\xi}_n^+ - \bar{z}_n\| = 0$, $\lim_{n\to-\infty} \|\bar{\xi}_n^- - \bar{z}_n\| = 0$ and the dichotomy assumption **A3** it follows from the Roughness-Theorem 10 that $\bar{z}_{\mathbb{Z}}$ has half-sided dichotomies on $\mathbb{Z}^-$ and on $\mathbb{Z}^+$. By the transversality assumption **A7** and [21, Proposition 2.6] we can combine these dichotomies and get an exponential dichotomy on $\mathbb{Z}$.

■

## 4.1 Construction of accurate boundary conditions

Let $Q_n^s$ and $Q_n^u$, $n \in \mathbb{Z}$ be the dichotomy projectors of (5). A sketch of heteroclinic trajectories and the stable and unstable subspaces of the exponential dichotomy at time $n_-$ and $n_+$ is given in Figure 5.

For the numerical approximation of $\bar{z}_{\mathbb{Z}}$ on the finite interval $J = [n_-, n_+]$, we demand the end points to lie in the green subspaces that are shifted to $\bar{\xi}_{n_-}$ and $\bar{\xi}_{n_+}$ in Figure 5. Formally, we require

$$z_{n_-} - \bar{\xi}_{n_-}^- \in \mathcal{R}(Q_{n_-}^u) \quad \text{and} \quad z_{n_+} - \bar{\xi}_{n_+}^+ \in \mathcal{R}(Q_{n_+}^s)$$

which is equivalent to

$$b_{n_\pm}(z_{n_-}, z_{n_+}) := \begin{pmatrix} (Y_{n_-}^1)^T (z_{n_-} - \bar{\xi}_{n_-}^-) \\ (Y_{n_+}^2)^T (z_{n_+} - \bar{\xi}_{n_+}^+) \end{pmatrix} = 0 \tag{18}$$

where $Y_{n_-}^1$ and $Y_{n_+}^2$ are bases of $\mathcal{R}(Q_{n_-}^u)^\perp$ and $\mathcal{R}(Q_{n_+}^s)^\perp$, respectively. Note that $Q_{n_-}^u$, $P_{n_-}^u$ as well as $Q_{n_+}^s$, $P_{n_+}^s$ converge exponentially fast towards each other.

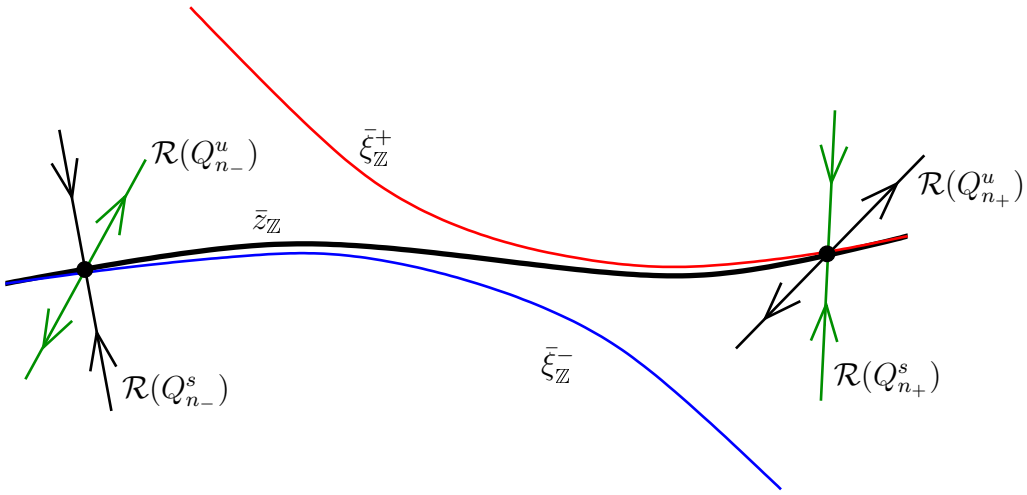


Figure 5: *Illustration of heteroclinic trajectories together with the corresponding stable and unstable subspaces at $n_-$ and $n_+$.*

Numerically, we compute dichotomy projectors $P^{-u}_{n_-}$ and $P^{+s}_{n_+}$ of the variational equations (3) and (4) at $n_-$ and $n_+$ using the algorithm that is proposed in [16] and [17], see Section 4.1.1. This task first requires the approximation of $\bar{\xi}^-_{\mathbb{Z}}$ and $\bar{\xi}^+_{\mathbb{Z}}$ on buffer intervals $[n^1_-, n^2_-]$ and $[n^1_+, n^2_+]$ around $n_-$ and $n_+$, using the techniques from Section 3, see Figure 6. If the buffer intervals are sufficiently large, we obtain in this way also good approximations of $Q^u_{n_-}$ and $Q^s_{n_+}$.

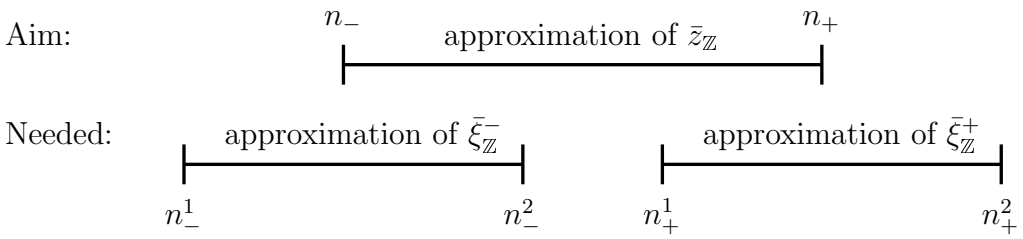


Figure 6: *Construction of buffer intervals for computing accurate boundary conditions.*

### 4.1.1 Computing dichotomy projectors

We illustrate the computation of the dichotomy projector $P^{+s}_{n_+}$, if an approximate trajectory $\xi^+_n$ for $n \in [n^1_+, n^2_+]$ is given. For this task the following least squares approach from [17] applies.

Let $P = B^+R$ with Moore-Penrose inverse $B^+ = B^T(BB^T)^{-1}$, where

$$B = \begin{pmatrix} -A_{n_+^1} & I & & & \\ & \ddots & \ddots & & \\ & & \ddots & \ddots & \\ & & & -A_{n_+^2-1} & I \end{pmatrix}, \quad A_n = D_x f(\xi_n^+, \bar{\lambda}_n),$$

and the $i$-th block $R_{[i]}$ of the matrix $R \in \mathbb{R}^{k(n_+^2 - n_+^1),k}$ is given as

$$R_{[i]} = \begin{cases} 0 & \text{for } i = n_+^1, \ldots, n_+^2 - 1,\ i \neq n_+ - 1, \\ I & \text{for } i = n_+ - 1. \end{cases}$$

Then the rows from $k(n_+ - n_+^1)+1$ to $k(n_+ - n_+^1+1)$ of $P$ form an approximation $\tilde{P}_{n_+}^{+s}$ of dichotomy projector $P_{n_+}^{+s}$. Similarly, we compute $\tilde{P}_{n_-}^{-u} = I - \tilde{P}_{n_-}^{-s}$.

Note that instead of computing the inverse of $BB^T$ one solves the linear system $BB^Tw = R$ and gets $P = B^Tw$. Further note that the error of the projector approximation shrinks exponentially fast in $n_\pm - n_\pm^1$ and $n_\pm^2 - n_\pm$, see [17, Theorem 4].

## 4.2 Approximation theorem for heteroclinic trajectories

Combining the previous results, we get the following approximation theorem for heteroclinic trajectories.

**Theorem 8** *Assume **A1**-**A7**. Then there exist positive constants $\delta, N$ such that the boundary value problem* (2), (18) *has a unique solution*

$$z_J \in B_\delta(\bar{z}_J), \quad \text{for } -n_-, n_+ > N.$$

*With a $J$-independent constant $C > 0$, the error can be estimated as*

$$\|\bar{z}_J - z_J\| \leq C\|b_{n_\pm}(\bar{z}_{n_-}, \bar{z}_{n_+})\|. \tag{19}$$

**Proof:** From Theorem 6, we obtain for sufficiently large buffer intervals accurate approximations of the semi-bounded trajectories $\bar{\xi}_{\mathbb{Z}}^-$ and $\bar{\xi}_{\mathbb{Z}}^+$ on $[n_-^1, n_-^2]$ and on $[n_+^1, n_+^2]$, respectively. Furthermore, accurate approximations of the corresponding dichotomy projectors of the variational equations (3), (4) at $n_-$ and $n_+$ can be computed, using the above algorithm. The boundary operator

$$b_{n_\pm}(\bar{z}_{n_-}, \bar{z}_{n_+}) = \begin{pmatrix} (Y_{n_-}^1)^T(\bar{z}_{n_-} - \xi_{n_-}^-) \\ (Y_{n_+}^2)^T(\bar{z}_{n_+} - \xi_{n_+}^+) \end{pmatrix}$$

converges to 0 as $n_\pm \to \pm\infty$, where $Y_{n_-}^1$ and $Y_{n_+}^2$ are bases of the numerically computed subspaces $\mathcal{R}(\tilde{P}_{n_-}^{-u})^\perp$ and $\mathcal{R}(\tilde{P}_{n_+}^{+s})^\perp$, and the matrix

$$\begin{pmatrix} D_1 b_{n_\pm}(\bar{z}_{n_-}, \bar{z}_{n_+})_{|\mathcal{R}(Q_{n_-}^s)} & D_2 b_{n_\pm}(\bar{z}_{n_-}, \bar{z}_{n_+})_{|\mathcal{R}(Q_{n_+}^u)} \end{pmatrix}$$

has a uniformly bounded inverse. Consequently, Appendix B, Theorem 11 applies and guarantees uniqueness of the boundary value solution in $B_\delta(\bar{z}_J)$ as well as the error estimate (19).

■

## 4.3 Numerical experiments: Computation of heteroclinic trajectories

We revisit the example from Section 3.3 and compute a heteroclinic trajectory with respect to the two families of semi-bounded trajectories that are given in Figure 4. For this task, we first choose two semi-bounded trajectories $\xi_{\mathbb{Z}}^{\pm}(\lambda_{\mathbb{Z}})$ on the interval $[-100, 0]$ and $[0, 100]$, respectively. Then, we approximate accurate projection boundary conditions at $n_- = -50$ and $n_+ = 50$, using the least squares approach from Section 4.1.1. Finally, we solve the obtained boundary value problem (2), (18) on the interval $[-50, 50]$. The resulting orbit, and two families of semi-bounded trajectories are shown in Figure 7.

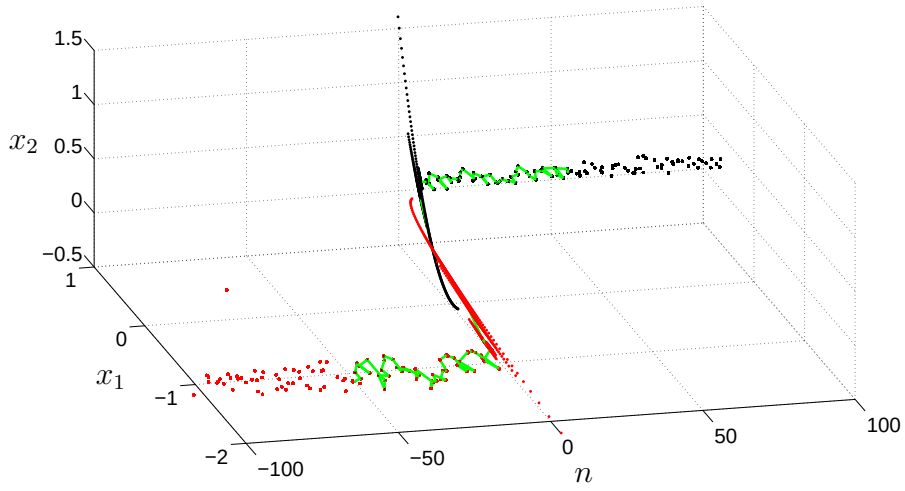


Figure 7: *Two families of semi-bounded trajectories (in red and black) and a heteroclinic connection of these families (in green).*

For solving our boundary value problem (2), (18) we use Newton's method. As initial guess, we choose the corresponding points of the semi-bounded trajectories on $[-50, -1]$ and $[1, 50]$, respectively, as well as an appropriate midpoint at 0. Obviously, the choice of this initial guess and particularly of the midpoint influences whether the heteroclinic orbit lies in the primary intersection of the stable and unstable fiber bundle at 0 (denoted by $P$ in Figure 4) or in secondary intersections that are not shown in our diagrams. For two different midpoints,

the resulting orbits are given in Figure 8. One observes that the green orbit in Figure 8 lies in the primary intersection $P$ of the stable and unstable fiber, while the blue orbit must lie in a secondary intersection.

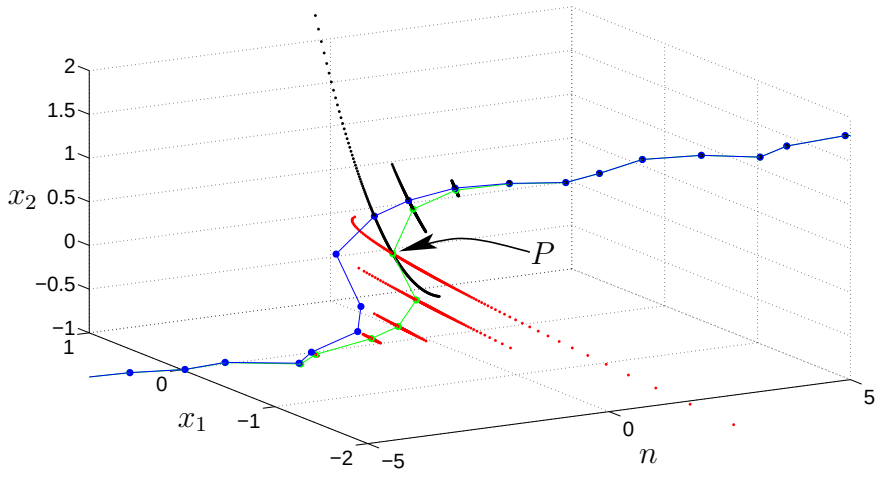


Figure 8: *Two heteroclinic trajectories (in green and blue) that are computed for two different initial values of Newton's method. Additionally, two families of semi-bounded trajectories are shown (in red and black) .*

# A Exponential dichotomy

In this appendix, we collect some well known results on exponential dichotomies from [21].

Denote by $\Phi$ the solution operator of the linear difference equation

$$u_{n+1} = A_n u_n, \quad A_n \in \mathbb{R}^{k,k} \text{ invertible }, \quad n \in \mathbb{Z}, \tag{20}$$

which is defined as

$$\Phi(n,m) := \begin{cases} A_{n-1} \dots A_m & \text{for } n > m, \\ I & \text{for } n = m, \\ A_n^{-1} \dots A_{m-1}^{-1} & \text{for } n < m. \end{cases}$$

**Definition 9** *The linear difference equation* (20) *has an* ***exponential dichotomy*** *with data* $(K, \alpha_s, \alpha_u, P_n^s, P_n^u)$ *on* $J \subset \mathbb{Z}$*, if there exist two families of projectors* $P_n^s$ *and* $P_n^u = I - P_n^s$ *and constants* $K,\ \alpha > 0$*, such that the following statements hold:*

$$P_n^s \Phi(n,m) = \Phi(n,m) P_m^s \quad \forall n, m \in J,$$

$$\begin{aligned} \|\Phi(n,m)P_m^s\| &\leq Ke^{-\alpha_s(n-m)} \\ \|\Phi(m,n)P_n^u\| &\leq K\mathrm{e}^{-\alpha_u(n-m)} \end{aligned} \qquad \forall n \geq m,\ n,m \in J.$$

We introduce an important perturbation result for exponential dichotomies, frequently named as Roughness-Theorem, cf. [5].

**Theorem 10** *Assume that the difference equation*

$$u_{n+1} = A_n u_n, \quad A_n \in \mathbb{R}^{k,k} \text{ invertible}, \quad \|A_n^{-1}\| \leq M \ \forall n \in J$$

*with $J \subseteq \mathbb{Z}$, has an exponential dichotomy with data $(K, \alpha_s, \alpha_u, P_n^s, P_n^u)$. There exits a constant $\beta > 0$ such that for $0 < \delta < \min(\alpha_s, \alpha_u)$ and $B_n \in \mathbb{R}^{k,k}$ satisfying $\|B_n\| \leq \beta$ for all $n \in J$, the matrix $A_n + B_n$ is invertible and the perturbed difference equation*

$$u_{n+1} = (A_n + B_n)u_n$$

*has an exponential dichotomy on $J$ with data $\big(\hat{K}, \alpha_s - \delta, \alpha_u - \delta, Q_n^s, Q_n^u\big)$, where $\operatorname{rank}(Q_n^s) = \operatorname{rank}(P_n^s)$ and*

$$\|P_n^s - Q_n^s\| \leq 2K^2 \frac{1 + \mathrm{e}^{-\alpha}}{1 - \mathrm{e}^{-\alpha}} \sup_{m \in J} \|B_m\| \quad \text{for all } n \in J.$$

# B Approximation theorem for bounded trajectories

We state a fundamental approximation result [18, Theorem 4] for bounded trajectories in this appendix.

**Theorem 11** *Assume **A1** and let $\bar{\mu}_{\mathbb{Z}}$ be a sequence of parameters such that $x_{n+1} = f(x_n, \bar{\mu}_n)$, $n \in \mathbb{Z}$ has a bounded solution $\bar{\zeta}_{\mathbb{Z}}$. Further assume that the variational equation*

$$u_{n+1} = D_x f(\bar{\zeta}_n, \bar{\mu}_n)u_n, \quad n \in \mathbb{Z}$$

*has an exponential dichotomy on $\mathbb{Z}$ with projectors $P_n^{s,u}$.*

*Let $b_{n_\pm} \in C^1(\mathbb{R}^{2k}, \mathbb{R}^k)$ be a boundary condition such that $Db_{n_\pm}(x_{n_-}, x_{n_+})$ is uniformly bounded and uniformly Lipschitz for all $x_{\mathbb{Z}} \in U$ and all $n_-$, $n_+$ with sufficiently large $n_+ - n_-$. Here $U$ is some fixed neighborhood of $\bar{\zeta}_{\mathbb{Z}}$. Assume that*

$$b_{n_\pm}(\bar{\zeta}_{n_-}, \bar{\zeta}_{n_+}) \to 0 \quad \text{as } n_\pm \to \pm\infty,$$

*and that the matrix*

$$\Big(D_1 b_{n_\pm}(\bar{\zeta}_{n_-}, \bar{\zeta}_{n_+})_{|\mathcal{R}(P^s_{n_-})} \quad D_2 b_{n_\pm}(\bar{\zeta}_{n_-}, \bar{\zeta}_{n_+})_{|\mathcal{R}(P^u_{n_+})}\Big)$$

*has a uniformly bounded inverse.*

*Then constants $\delta$, $N$ exist, such that the boundary value problem*

$$\begin{aligned} x_{n+1} &= f(x_n, \bar{\mu}_n), \quad n = n_-, \ldots, n_+ - 1, \\ b_{n_\pm}(x_{n_-}, x_{n_+}) &= 0 \end{aligned}$$

*has a unique solution*

$$x_J \in B_\delta(\bar{\zeta}_J) \quad \textit{for } J = [n_-, n_+],\ -n_-,\ n_+ \geq N.$$

*With a $J$-independent constant $C > 0$, the error can be estimated as*

$$\|\bar{\zeta}_J - x_J\| \leq C \|b_{n_\pm}(\bar{\zeta}_{n_-}, \bar{\zeta}_{n_+})\|.$$

# References


[1] W.-J. Beyn. The numerical computation of connecting orbits in dynamical systems. *IMA J. Numer. Anal.*, 10:379–405, 1990.

[2] W.-J. Beyn and T. Hüls. Error estimates for approximating non-hyperbolic heteroclinic orbits of maps. *Numer. Math.*, 99(2):289–323, 2004.

[3] W.-J. Beyn, T. Hüls, J.-M. Kleinkauf, and Y. Zou. Numerical analysis of degenerate connecting orbits for maps. *Internat. J. Bifur. Chaos Appl. Sci. Engrg.*, 14(10):3385–3407, 2004.

[4] W.-J. Beyn, T. Hüls, and M.-C. Samtenschnieder. On $r$-periodic orbits of $k$-periodic maps. *J. Difference Equ. Appl.*, 14(8):865–887, 2008.

[5] W.-J. Beyn and J.-M. Kleinkauf. The numerical computation of homoclinic orbits for maps. *SIAM J. Numer. Anal.*, 34(3):1207–1236, 1997.

[6] R. L. Devaney. *An Introduction to Chaotic Dynamical Systems*. Addison-Wesley Studies in Nonlinearity. Addison-Wesley Publishing Company Advanced Book Program, Redwood City, CA, second edition, 1989.

[7] A. Dhooge, W. Govaerts, and Y. A. Kuznetsov. MATCONT: a MATLAB package for numerical bifurcation analysis of ODEs. *ACM Trans. Math. Software*, 29(2):141–164, 2003.

[8] S. Elaydi and R. J. Sacker. Global stability of periodic orbits of non-autonomous difference equations and population biology. *J. Differential Equations*, 208(1):258–273, 2005.

[9] S. Elaydi and R. J. Sacker. Nonautonomous Beverton-Holt equations and the Cushing-Henson conjectures. *J. Difference Equ. Appl.*, 11(4-5):337–346, 2005.

[10] R. K. Ghaziani, W. Govaerts, Y. A. Kuznetsov, and H. G. E. Meijer. Numerical continuation of connecting orbits of maps in MATLAB. *J. Difference Equ. Appl.*, 15(8-9):849–875, 2009.

[11] J. K. Hale and H. Koçak. *Dynamics and Bifurcations*, volume 3 of *Texts in Applied Mathematics*. Springer-Verlag, New York, 1991.

[12] M. Hénon. A two-dimensional mapping with a strange attractor. *Comm. Math. Phys.*, 50(1):69–77, 1976.

[13] M. W. Hirsch, C. C. Pugh, and M. Shub. *Invariant manifolds*. Springer-Verlag, Berlin, 1977. Lecture Notes in Mathematics, Vol. 583.

[14] T. Hüls. Bifurcation of connecting orbits with one nonhyperbolic fixed point for maps. *SIAM J. Appl. Dyn. Syst.*, 4(4):985–1007 (electronic), 2005.

[15] T. Hüls. Homoclinic orbits of non-autonomous maps and their approximation. *J. Difference Equ. Appl.*, 12(11):1103–1126, 2006.

[16] T. Hüls. Numerical computation of dichotomy rates and projectors in discrete time. *Discrete Contin. Dyn. Syst. Ser. B*, 12(1):109–131, 2009.

[17] T. Hüls. Computing Sacker-Sell spectra in discrete time dynamical systems. *SIAM J. Numer. Anal.*, 48(6):2043–2064, 2010.

[18] T. Hüls. Homoclinic trajectories of non-autonomous maps. *J. Difference Equ. Appl.*, 17(1):9–31, 2011.

[19] B. Krauskopf, H. M. Osinga, E. J. Doedel, M. E. Henderson, J. Guckenheimer, A. Vladimirsky, M. Dellnitz, and O. Junge. A survey of methods for computing (un)stable manifolds of vector fields. *Internat. J. Bifur. Chaos Appl. Sci. Engrg.*, 15(3):763–791, 2005.

[20] C. Mira. *Chaotic dynamics*. World Scientific Publishing Co., Singapore, 1987. From the one-dimensional endomorphism to the two-dimensional diffeomorphism.

[21] K. J. Palmer. Exponential dichotomies, the shadowing lemma and transversal homoclinic points. In *Dynamics reported, Vol. 1*, pages 265–306. Teubner, Stuttgart, 1988.

[22] C. Pötzsche and S. Siegmund. $C^m$-smoothness of invariant fiber bundles. *Topol. Methods Nonlinear Anal.*, 24(1):107–145, 2004.

[23] S. Smale. Differentiable dynamical systems. *Bull. Amer. Math. Soc.*, 73:747–817, 1967.

[24] S. Wiggins. *Normally hyperbolic invariant manifolds in dynamical systems*, volume 105 of *Applied Mathematical Sciences*. Springer-Verlag, New York, 1994. With the assistance of György Haller and Igor Mezić.